NON-DIMENSIONALISATION OF LATERAL DISTANCES BETWEEN VESSELS OF DISSIMILAR SIZES FOR INTERACTION EFFECT STUDIES

(DOI No: 10.3940/rina.ijme.2017.a4.429)

N Jayarathne, **D Ranmuthugala**, **Z Leong** and **J Fei**, Australian Maritime College, University of Tasmania, Australia

SUMMARY

To date, most of the hydrodynamic interaction studies between a tug and a ship during ship assist manoeuvers have been carried out using model scale investigations. It is however difficult to establish how well results from these studies represent full scale interaction behaviour. This is further exacerbated by the lack of proven methodologies to non-dimensionalise the relative distances between the two vessels, enabling the comparison of model and full scale interaction effect data, as well as between vessels of dissimilar size ratios. This study investigates a suitable correlation technique to non-dimensionalise the lateral distance between vessels of dissimilar sizes, and a scaling option for interaction effect studies. It focuses on the interaction effects on a tug operating around the forward shoulder of a tanker at different lateral distances during ship assist operations. The findings and the non-dimensioning method presented in this paper enable the interaction effects determined for a given ship-to-tug ratio to be used to predict the safe operational distances for other ship-to-tug ratios.

NOMENCLATURE

BR	Breadth Ratio, $BR = B_S/B_t$
B_s	Breadth of the tanker (m)
B_t	Breadth of the tug (m)
C_N	Yaw moment coefficient
C_X	Surge force coefficient
C_Y	Sway force coefficient
DR	Displacement Ratio, $(\nabla_s / \nabla_t)^{1/3}$
F_r	Length Froude Number, $F_r = u/\sqrt{g\ L_{WL}}$
g	Acceleration due to gravity (9.81 m s^{-2})
L_{OA}	Length overall of the tanker/tug (m)
L_s	Length waterline of the tanker (m)
L_t	Length waterline of the tug (m)
N	Yaw moment acting on tug (N m)
R_G	Mesh convergence ratio
T	Draft of the tanker/tug (m)
u	Fluid flow velocity (m s^{-1})
X	Surge force acting on tug (N)
Y	Sway force acting on tug (N)
y^+	Non-dimensional wall distance of first inflation layer
ΔX	Non-dimensionalised longitudinal-distance between vessels
δx	Longitudinal distance between vessels (m)
ΔY	Non-dimensionalised lateral distance between vessels
δy_{cl}	Lateral distance between vessels' centrelines (m)
δy_m	Lateral distance between vessels' midship (m)
ρ	Density of water (kg m^{-3})
∇_s	Volumetric displacement of the tanker (m^3)
∇_t	Volumetric displacement of the tug (m^3)

1. INTRODUCTION

Large ships operating at low speeds generally suffer from limited manoeuvrability, which can lead to dangerous situations in restricted or congested waters. Thus, in such situations, they are usually assisted by attending tugs, which exposes the smaller tugs to dangers such as collision, grounding, girting, and run-overs due to the hydrodynamic interaction effects between the two vessels (Hensen, 2012). The influence of hydrodynamic interaction is prominent when the comparative sizes of the two ships differ significantly, for example, when a tug operates near a large ship such as a large tanker or bulk carrier (Hensen, 2003). Furthermore, the effects of the interaction can change with the hull shapes of the ship and the tug, the width of the navigable channel in the river or harbour, the tug's location relative to the ship, the relative and absolute speeds of the two vessels, and the drift angle between them (Hensen, 2012).

When a ship is moving forward in calm water, it generates a pressure field around the hull. This results in a higher pressure around the bow region due to the retarded flow around the stagnation region in that area. The pressure reduces significantly around the mid-body section as the flow accelerates, which is followed by partial pressure recovery around the stern region. In the latter region, the adverse pressure gradient causes flow separation that results in a wake region around the stern and immediately aft of the hull. When vessels are operating in proximity to each other, the flow between the adjacent hulls can accelerate due to the limited space between them. This causes a low pressure region between the hulls (relative to the rest of the pressure field around the vessels) resulting in an attraction force between them, which in the case of a smaller tug can result in the tug colliding with, or being run over by, the larger ship. Conversely in the higher pressure regions such as the bow region of the ship, the smaller tug will experience a strong repulsive force that can adversely affect the tug's motion and orientation. Therefore, it is clear that the pressure field of the larger ship has a significant influence on the smaller ship when operating in close quarters, which needs to be investigated in order to

provide operators with information to avoid dangerous situations during ship assist operations.

To date, most of the interaction studies between vessels have been carried out for similar sized vessels (Chen & Fang, 2001, Falter, 2010, Fortson, 1974, Lataire et al., 2012, Lu et al., 2009, Newton, 1960, Pinkster & Bhawsinka, 2013, Tuck & Newman, 1974, Zou & Larsson, 2013), with only a small number targeting dissimilar sized vessels operating in close proximity (Dand, 1975, Fonfach *et al*., 2011, Geerts *et al*., 2011, Simonsen *et al*., 2011, Vantorre *et al*., 2002). Among them Dand (1975) conducted the pioneering Experimental Fluid Dynamics (EFD) based model scale study to investigate the dangers tug operators faced due to interaction effects while working in close proximity to large ships. The study used two different ship models and a single screw tug model at two different lateral distances between the ship and the tug. Dand (1975) concluded that if a tug can operate near the midship region of a larger ship, it experiences minimal interaction effects induced by the latter. Although his model scale findings provide tug operators with safe locations relative to the ship during ship assist manoeuvres, it is prudent to correlate it to full-scale scenarios and broaden the investigation to include various tug manoeuvres that occur during ship assist operations.

Vantorre *et al*. (2002) conducted model scale experiments to determine ship interaction effects for head-on and overtaking encounters of similar and dissimilar size ships and used the results to create a mathematical model to improve the realism of the interaction effects modelled within ship manoeuvring simulators. However, their model was unable to accurately represent the interaction effects generated between vessels of significant size difference, such as between a ship and a tug. Geerts *et al*. (2011) assessed the hydrodynamic interaction forces acting on a tug sailing freely in the vicinity of the bow of a larger ship through a series of model tests. The results were incorporated into a simulation program to assess the steering action of the tug required to counteract the ship's hydrodynamic effects in order to keep station relative to the ship. The authors do not provide any explanation on the extrapolation methodology employed to correlate the model scale results to full-scale vessel operations in order to represent actual ship-tug interaction manoeuvres. Simonsen *et al*. (2011) carried out a Computational Fluid Dynamics (CFD) study validated through model scale experiments to investigate quasi-steady interaction effects on a tug located at a number of positions parallel to a large tanker. Although they concluded that Reynolds Averaged Navier Stokes (RANS) based CFD simulations offer a promising tool for ship interaction studies, no information on the scaling effects on the interaction between the vessels were presented.

Among the literature available in the public domain, the study by Fonfach *et al*. (2011) is a notable contribution utilising full-scale CFD simulations to predict tug interaction effects. They used Froude scaling to compare full-scale CFD interaction effect coefficients with model scale EFD interaction effect coefficients for a tug located at various stations alongside a larger ship, with both vessels travelling at the same speed on parallel courses. The results revealed a relatively weak influence of viscosity on the interaction effects. Nevertheless, they expect the viscosity effects to be more pronounced in non-parallel operations, and when the tug is located within the ship's wake. They observed large discrepancies between their CFD and EFD results at small lateral clearances, especially for the sway force, although the cause of the discrepancies was not discussed. These discrepancies were possibly due to the lack of a comprehensive mesh independence study and the lack of a proven correlation technique to non-dimensionalise the vessel locations for comparison and scaling. The authors give no information on how the scaling issues between the model scale EFD and the full scale CFD were reconciled, which may have contributed to the differences between their results.

Most research studies available in the public domain (Dand, 1975, Fonfach *et al*., 2011, Geerts *et al*., 2011, Simonsen *et al*., 2011, Vantorre *et al*., 2002) do not explicitly describe or evoke a method to compare the interaction behaviour between a tug and a ship for different scales (for example to compare model scale results with full scale operations). With the exception of Fonfach *et al*. (2011), these studies utilised only model scale EFD investigations or model scale CFD simulations to investigate the interaction effects. Therefore, it is difficult to establish how well these model scale results represent full-scale interaction behaviours. This is further exacerbated by the lack of proven methodologies that can scale the relative model scale distances between the two vessels to full scale.

The work presented in this paper outlines an approach to non-dimensionalise lateral distances between vessels of dissimilar sizes to predict the interaction effects acting on a tug operating near large ships of different sizes or to correlate model scale and full scale interaction effects. It involves verification of the non-dimensionalising approaches for the lateral distances between vessels of different sizes and ratios. Previous work by the authors (Jayarathne *et al*., 2014) compared different numerical approaches (RANS based CFD vs Potential Flow) against experimental measurements to identify an accurate method to model the interaction effects between a tug and a ship. It was found that the CFD was the most accurate simulation technique to analyse non-streamlined bodies, although modelling and solution times can be significantly higher. This led to all future work being conducted with RANS based CFD, using StarCCM+®. CFD models were verified and validated at model scale using experimental measurements. Throughout the

analysis the tug was maintained within the forward shoulder of the ships, which according to Dand (1975) is the most hazardous region for a tug to operate. The findings enable tug operators to familiarise themselves with the relationship between the hydrodynamic interaction effects and the lateral distances between dissimilar sized vessels.

2. CASE STUDY

Figure 1 shows the four cases including the model scale investigations used in this study to identify a suitable approach to non-dimensionalise the lateral distances between two vessels of dissimilar size. The dimensions of the smaller vessel geometry, i.e. the stern drive tug, was kept fixed, while the larger ship geometry, i.e. the MARAD-F series tanker, was scaled to obtain the different breadth ratios (*BR*), defined as the tanker breadth (B_s) to the tug breadth (B_t) as shown in eqn. 1.

$$BR = \frac{B_S}{B_t} \tag{1}$$

Full scale CFD simulations were carried out for all the breadth ratios, while model scale CFD simulations were carried at a breadth ration of 1.14 to enable validation against experimental data. The tanker and tug particulars for the different scales and breath ratios are outlined in Table 1. These breadth ratios were selected based on the most common dimensions of the small to medium size ships and tugs currently operational in international waters (Artyszuk, 2013).

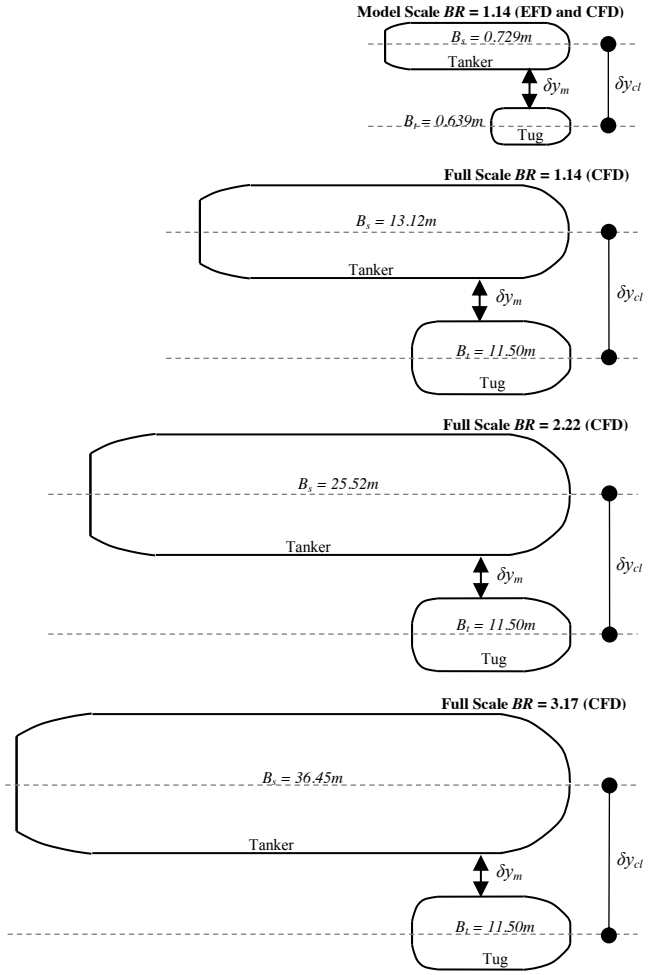

Figure 1: Different Ship Breadth Ratios (*BR*) investigated within the study showing the distance between ships' centrelines (δy_{cl}) and the distance between ships' midship (δy_m). *Not to scale*.

Table 1. Principal particulars of the selected hull forms.

Scale type		Model Scale		Full Scale		Full Scale		Full Scale	
Breadth Ratio (*BR*)		1.14		1.14		2.22		3.17	
Displacement Ratio (*DR*)		1.12		2.42		4.70		6.72	
Analysis type		EFD and CFD		CFD		CFD		CFD	
Main Particulars	Unit	Tanker	Tug	Tanker	Tug	Tanker	Tug	Tanker	Tug
Length Overall (L_{OA})	m	4.200	1.732	75.60	31.16	147.00	31.16	210.00	31.16
Length Waterline (L_s *or* L_t)	m	4.000	1.581	72.00	28.46	140.00	28.46	200.00	28.46
Breadth (B_s *or* B_t)	m	0.729	0.639	13.12	11.50	25.52	11.50	36.45	11.50
Draft (T)	m	0.246	0.197	4.42	4.50	8.61	4.50	12.30	4.50
Scale	-	1	1	18	18	35	18	50	18
Froude number (Length) $u/(\sqrt{gL_{wl}})$	-	0.065	0.104	0.065	0.104	0.047	0.104	0.039	0.104
Froude number (Depth) $u/(\sqrt{gD})$	-	0.146		0.146		0.146		0.146	
Speed (u)	m/s	0.41		1.74		1.74		1.74	

Figure 2 shows the local (tug) and global coordinate systems used for the spatial, force, and moment references. Throughout the analysis the tug was located on the port side of the tanker. The approaches used to non-dimensionalise the lateral distance and that for the longitudinal distances are given in eqns. 2, 3, and 4 respectively.

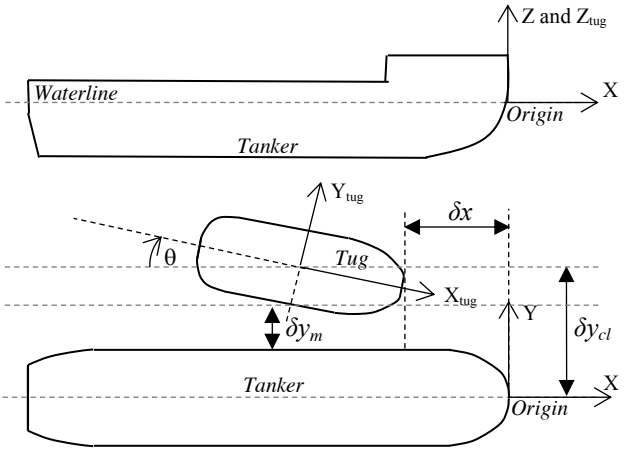

Figure 2: Local (tug) and global coordinate systems and vessel locations.

$$\Delta Y_{ship} = \frac{\delta y_{cl}}{B_s} \quad (2)$$

$$\Delta Y_{tug} = \frac{\delta y_{cl}}{B_t} \quad (3)$$

$$\Delta X = \frac{2\delta x}{L_s} \quad (4)$$

The ratio ΔY_{ship} is the non-dimensionalised lateral distance between the vessels calculated as a ratio of the tanker breadth (i.e. large ship breadth). ΔY_{tug} is the same however, calculated as a ratio of the tug breadth. ΔX is the non-dimensionalised longitudinal distance between two ship bows.

The tug was located at the forward shoulder of the tanker throughout the analysis, maintaining $\delta x = 0$, and therefore the non-dimensionalised longitudinal distance was zero, i.e. $\Delta X = 0$. The tug drift angle (θ) was maintained as zero degrees throughout the analysis representing parallel vessel operations.

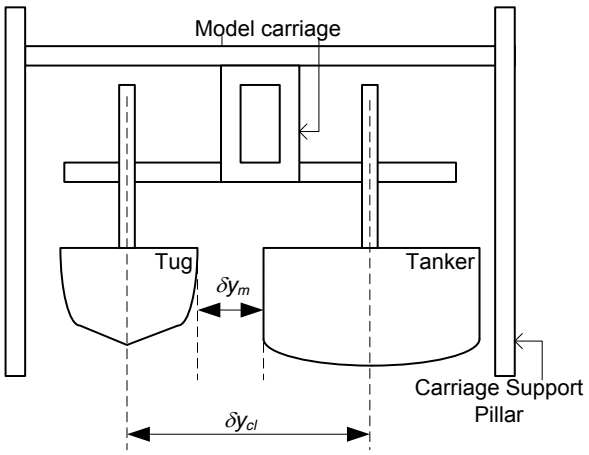

Figure 3: Schematic of the experimental setup in AMC's Model Test Basin.

As seen in Figure 3, due to the limited distance between the carriage support pillars in the experiment, only two cases representing different lateral distances between the midship of hull models (δy_{m_1} and δy_{m_2}) of 0.913m and 0.975m were used in the study. For each of the above cases, the lateral distances between ship centrelines (δy_{cl}) were measured as δy_{cl_1}= 1.597m and δy_{cl_2}= 1.659m respectively.

Table 2. Lateral distances between vessel centrelines (δy_{cl}).

Lateral distances between vessel centrelines (δy_{cl}) calculated based on;		Model Scale *BR* = 1.14	Full Scale *BR* = 1.14	Full Scale *BR* = 2.22	Full Scale *BR* = 3.17
		δy_{cl} (m)	δy_{cl} (m)	δy_{cl} (m)	δy_{cl} (m)
		EFD and CFD	CFD	CFD	CFD
1	δy_{m_1} = 0.913m	1.597	13.22	19.42	24.89
2	ΔY_{ship_1} = 2.190	1.597	28.75	55.89	79.85
3	ΔY_{tug_1} = 2.499	1.597	28.74	28.74	28.74
4	δy_{m_2}= 0.975m	1.659	13.27	19.48	24.95
5	ΔY_{ship_2}= 2.276	1.659	29.86	58.06	82.95
6	ΔY_{tug_2}= 2.596	1.659	29.86	29.86	29.86

The first of the approaches to represent lateral distance between ship and tug used the absolute distance between the two hulls (δy_m) that was maintained as per the experimental distances at δy_{m_1}= 0.913m and δy_{m_2}= 0.975m. This enabled a comparison between the approaches using the absolute distance and the two non-dimensional distances given in eqns. 2 and 3. For the second approach, the lateral distance between the vessel centrelines (δy_{cl}) was calculated by eqn. 2 using the same non-dimensionalised distance (ΔY_{ship}), which was determined from the model scale vessel dimensions and set-up. The last approach was similar, except for the use of eqn. 3 for non-dimensioning the lateral distances. A summary of the distances calculated for the three approaches is given in Table 2.

The surge force (X), sway force (Y), and yaw moment (N) acting on the tug for different cases were measured and non-dimensionalised using volumetric displacements according to eqns. 5 to 7 (Fonfach *et al*., 2011, Simonsen *et al*., 2011) respectively.

$$C_X = \frac{2X}{u^2 \nabla_t^{1/3} \nabla_s^{1/3} \rho} \tag{5}$$

$$C_Y = \frac{2Y}{u^2 \nabla_t^{1/3} \nabla_s^{1/3} \rho} \tag{6}$$

$$C_N = \frac{2N}{u^2 \nabla_t^{1/3} \nabla_s^{1/3} L_t \rho} \tag{7}$$

where;

C_N Yaw moment coefficient
C_X Surge force coefficient
C_Y Sway force coefficient
L_t Length waterline of the tug (m)
u Fluid flow velocity (m s^{-1})
ρ Density of water (kg m^{-3})
∇_s Volumetric displacement of the tanker (m^3)
∇_t Volumetric displacement of the tug (m^3)

3. CFD SETUP

The commercial CFD code, Star-CCM+® was used to investigate the test scenarios outlined in Table 2 via Reynolds Averaged Navier-Stokes (RANS)-based simulations. Model scale CFD simulations replicated the experimental captive model test conditions to enable the validation of the CFD models. The validated model was then scaled up to full scale using Froude scaling technique to create the full scale CFD simulation domains (see Figure 4). Local mesh refinements were carried out to maintain the y^+ value and to improve the quality and the stability of the simulations. Both the tanker and tug geometries were fixed within the domain, i.e. with zero degrees of freedom.

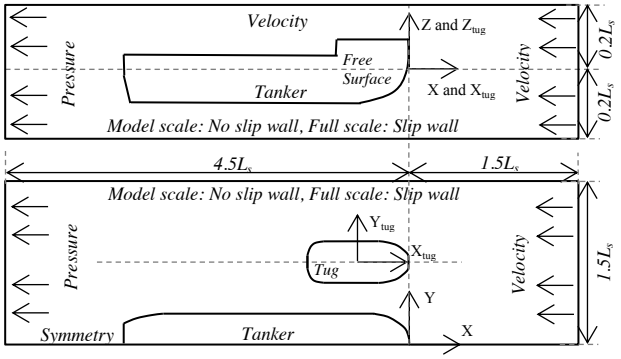

Figure 4: Computational domain used in Star-CCM+® simulations.

The upstream end and top boundaries of the domain were kept as inlet boundaries, while the downstream end was maintained as a pressure outlet. The velocity inlet at the top boundary was used in preference to a slip wall boundary to reduce the simulation convergence time without affecting the accuracy of results (CD-Adapco, 2015). A symmetry boundary along the longitudinal mid-plane of the tanker, as used by Fonfach (2010), was employed in this study to significantly reduce the computational effort by reducing the size of the mesh domain. As the domain is not symmetric about the x-y plane due to the placement of the tug on the Port bow of the tanker, it was required to verify that the use of a symmetry plane resulted in minimum errors on the forces and moments calculated. This was carried out by comparing the results between a domain utilising the symmetry plane geometry as shown in Figure 4 against a compatible full domain simulation. The maximum difference between the forces and moments obtained for the two simulation domains were within 0.5% of each other and were thus deemed negligible for the current study. The free surface in the CFD simulation was modelled as an Euler Multiphase using the volume of fluid (VOF) technique. The turbulence was modelled with a Shear Stress Transport (SST) turbulence model, which enabled the closure of the RANS equations.

4. EFD SETUP

Experimental captive model testing was conducted in the AMC's 35m (length) x 12m (width) x 1.0m (depth) Model Test basin to validate the CFD model. It was equipped with a multi model carriage mechanism (Figure 5). Tanker and tug models of 1:18 scale were attached to the carriage by keeping them fixed in all degrees of freedom and without allowing relative motion at their fully loaded drafts. The tug model was connected using two strain gauges to measure the surge and sway forces and to calculate the yaw moment. The tanker model was attached to the carriage without strain gauges, since this study focused on the interaction effects on the smaller tug hull due to the relative size difference in typical tug assist operations. Experimental uncertainty limits were calculated in accordance with the ITTC (2002) giving 7%, 9.4%, and 7% for the interaction surge force, sway force, and yaw moment respectively (Jayarathne *et al*., 2017).

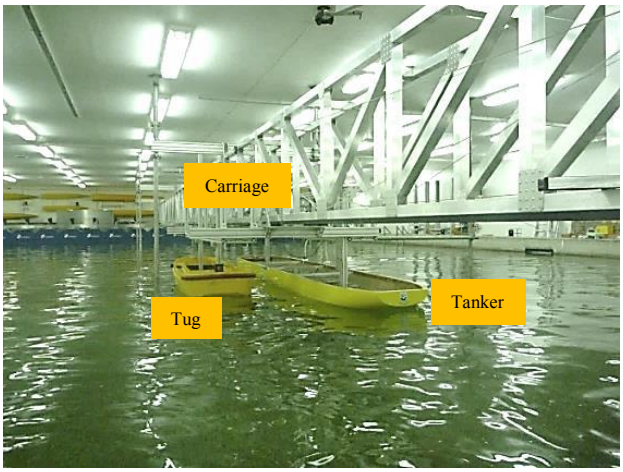

Figure 5: Experimental setup to measure the interaction effects between vessels in AMC's Model Test Basin.

5. CFD VERIFICATION AND VALIDATION

5.1 MESH SENSITIVITY STUDY

A suitable mesh for simulation was identified by evaluating the effects of the mesh resolution. As stated by Fonfach *et al*. (2011), the study carried out by the authors in Jayarathne *et al*. (2017) showed that it is required to resolve the boundary layer in order to accurately model the hydrodynamic interaction effects on a tug that is operating in close proximity to a larger vessel and at an angle of drift to the latter. Therefore, the initial (base) mesh setting had a nominal total inflation layer thickness of two times Prandtl's 1/7th power law turbulent boundary layer thickness estimate ($2x0.16L_t/Re_{Lt}^{1/7}$), while a first layer y^+ of 1 were applied around the vessels. The authors provide more information on these selections and mesh refinement in Jayarathne *et al*., (2017) and Leong *et al*., (2014). In order to determine the uncertainty of the mesh resolution selected, mesh sensitivity studies for the model and full scale mesh domains were conducted using the Richardson Extrapolation method (Stern *et al*., 2001).

The mesh models were generated by Star-CCM+®'s built in mesh generator using an unstructured hexahedral mesh approach. For each model and full scale breadth ratio, three mesh models: fine, medium and coarse were created with an approximate refinement ratio of $\sqrt{2}$ (see Table 3). The relevant mesh refinements were carried out on the vessel surfaces and in the pressure regions around the vessels.

Table 3. Mesh resolution of the simulations used for the sensitivity study (M – Millions).

Mesh (Number)	Fine (1)	Medium (2)	Coarse (3)
Model Scale *BR* = 1.14	7.2M	4.8M	3.5M
Full Scale *BR* = 1.14	12.3M	8.7M	6.0M
Full Scale *BR* = 2.22	13.2M	9.2M	6.8M
Full Scale *BR* = 3.17	14.6M	10.9M	7.6M

Mesh convergence ratios (R_G, given in eqn. 8) for the surge force, sway force, and yaw moment for all the conditions were within $0<R_G<1$, and thus monotonic convergence was deemed to be achieved (Stern *et al*., 2001).

$$R_G = \frac{\epsilon_{21}}{\epsilon_{32}} \tag{8}$$

where ϵ_{21} is the change in the results between the fine and medium mesh while ϵ_{32} is the change between the medium and coarse mesh.

Numerical errors for the selected mesh models were calculated in accordance with the procedure described by Stern *et al*. (2001), with errors calculated for the surge and sway forces and the yaw moment presented in Table 4. The error percentage estimates in comparison to the Richardson extrapolated values (Stern *et al*., 2001) for the fine mesh models were below the experimental uncertainties, thus providing sufficient accuracy for the cases investigated in the current study. As mentioned previously, the y^+ value was maintained below 1, with information on the y^+ study given in Jayarathne *et al*. (2017). The fine mesh models selected for the remainder of this study are shown in Figure 6.

Table 4. Relative error percentage estimates of the surge and sway forces and the yaw moment with respect to the Richardson extrapolated values.

Interaction Effect	Percentages (%) of the relative error estimates								
	Surge Force			Sway Force			Yaw Moment		
Mesh Number	1	2	3	1	2	3	1	2	3
Model scale *BR* = 1.14	0.43	1.44	4.78	1.96	3.89	7.55	1.21	2.53	5.24
Full Scale *BR* = 1.14	0.81	4.99	10.38	5.08	9.83	13.34	2.09	4.51	12.26
Full Scale *BR* = 2.22	0.98	3.25	8.73	5.12	8.41	14.09	5.35	7.88	14.44
Full Scale *BR* = 3.17	0.41	2.10	6.87	2.09	5.99	9.12	3.56	6.64	13.25

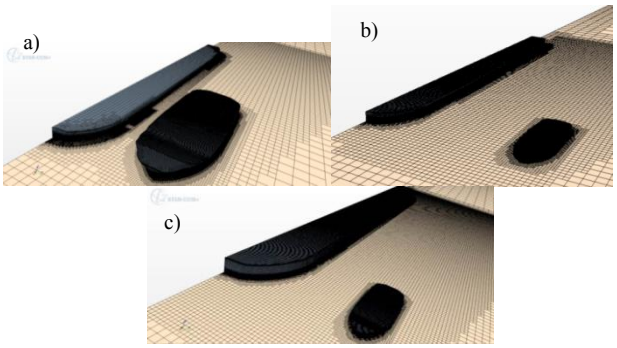

Figure 6: Selected mesh models a) Full Scale *BR* = 1.14, b) Full Scale *BR* = 2.22, Full Scale *BR* = 3.17.

5.2 CFD VALIDATION AGAINST EFD MEASUREMENTS

Figure 7 shows the comparison of model scale EFD, model scale CFD, and full scale CFD interaction effects on a tug for *BR* = 1.14 at two non-dimensioned lateral distances, i.e. ΔY_{ship}= 2.190 and ΔY_{ship}= 2.276. It compares the CFD predicted interaction surge and sway forces and yaw moment acting on the tug at different lateral distances against the EFD measurements.

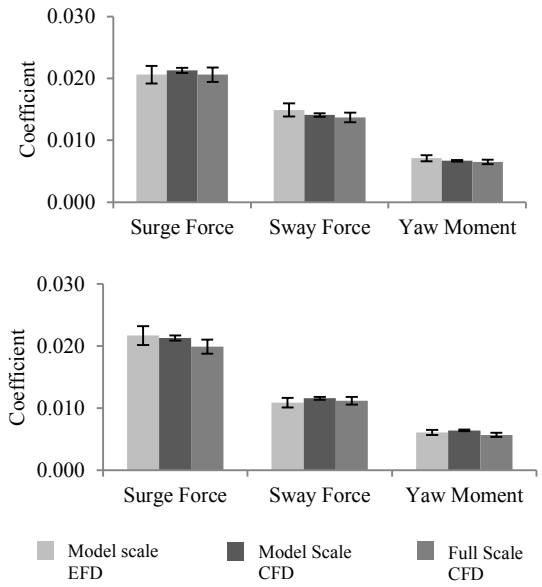

Figure 7: Interaction effect coefficients obtained through model scale EFD, model scale CFD and full scale CFD for the tug for *BR* = 1.14, a) ΔY_{ship} = 2.190 and b) ΔY_{ship} = 2.276. Error bars represent the respective CFD and EFD uncertainties.

The model scale CFD and model scale EFD results are in good agreement, with the difference being less than the experimental uncertainty, i.e. 7%, 9.4%, and 7% for the surge force, sway force, and yaw moment respectively. The model scale and full-scale predictions were in good agreement (within 8%) thus providing confidence for the CFD model to be extended to full scale conditions. However, it is important to note that the agreement between these results was not validated using full scale experimental results. This was due to the absence of such data or studies conducted to investigate full scale interaction effects.

6. RESULTS DISCUSSION

This section discusses the surge and sway forces and yaw moment coefficients on the tug when positioned alongside three different tankers at different lateral distances, as explained in Section 2. It compares the methods used to scale lateral distances between vessels of dissimilar sizes. This is followed by the characterisations of the flow field around the vessels using pressure visualisation.

6.1 COMPARISON OF METHODS USED TO CALCULATE LATERAL DISTANCES

Figure 8 illustrates the interaction effect coefficients (eqns. 5 to 7) of the tug. These were determined through different lateral distance calculation methods (δy_m, ΔY_{ship} and ΔY_{tug}, i.e. the absolute distance and the non-dimensional distances given in eqns. 2 and 3) with the different full scale breadth ratios (i.e. *BR* = 1.14, 2.22, 3.17) investigated in this study. Two lateral distances are presented for each of the methods to verify the behaviour on the interaction effects between different sized vessels.

When using absolute lateral distance (δy_m) to represent the distance between vessels, the forces and moment coefficients changed substantially with changing breath ratios (Figure 8). As seen in the figure, the sway force showed a significant decline in contrast to the yaw moment, which showed a rapid increase with the increasing breadth ratio. The discrepancies of the results between the breadth ratios were 268%, 44%, and 13% for the yaw moment, sway force, and surge force coefficients respectively. These discrepancies were far beyond the experimental and numerical uncertainties, and thus using the absolute distance is unsuitable for scaling and comparing the hydrodynamic interaction effects between vessels of different sizes. This would be expected, as the absolute distance disregards the size of the vessels.

Next consider the results using the non-dimensionalised lateral distance based on the tug breadth, i.e. ΔY_{tug}. At a $\Delta Y_{tug_1}$of 2.499, the discrepancies were up to 9%, 41%, and, 11% for surge force, sway force and yaw moment coefficients respectively between the three breadth ratios. At ΔY_{tug_2}= 2.596, the discrepancies were also found to be substantial with 23%, 35%, and, 2% differences for surge force, sway force and yaw moment respectively between the breadth ratios. As seen in Figure 8, except for the sway force at $\Delta Y_{tug_2}$and yaw moment at ΔY_{tug_1}, the rest of the cases showed that the maximum discrepancies were at the breadth ratio of 3.17. Although it is hard to define

an exact pattern in the results, it is apparent that the discrepancies were mainly affected by the increase in the breadth ratio. Thus, the non-dimensionalising method using the ΔY_{tug} is also unsuitable as the discrepancies in the results is not consistent between the two lateral distances and still exceeds EFD and CFD uncertainties. The weakness of the ΔY_{tug} approach is that it uses only the tug's breadth (B_t) to non-dimensionalise the lateral distance, thus neglecting dimensions of the larger ship. Thus, a scaling that solely uses the tug's breadth is deemed insufficient to represent the required lateral distances for the tug to experience similar interaction effects when operating in close proximity to ships of different sizes.

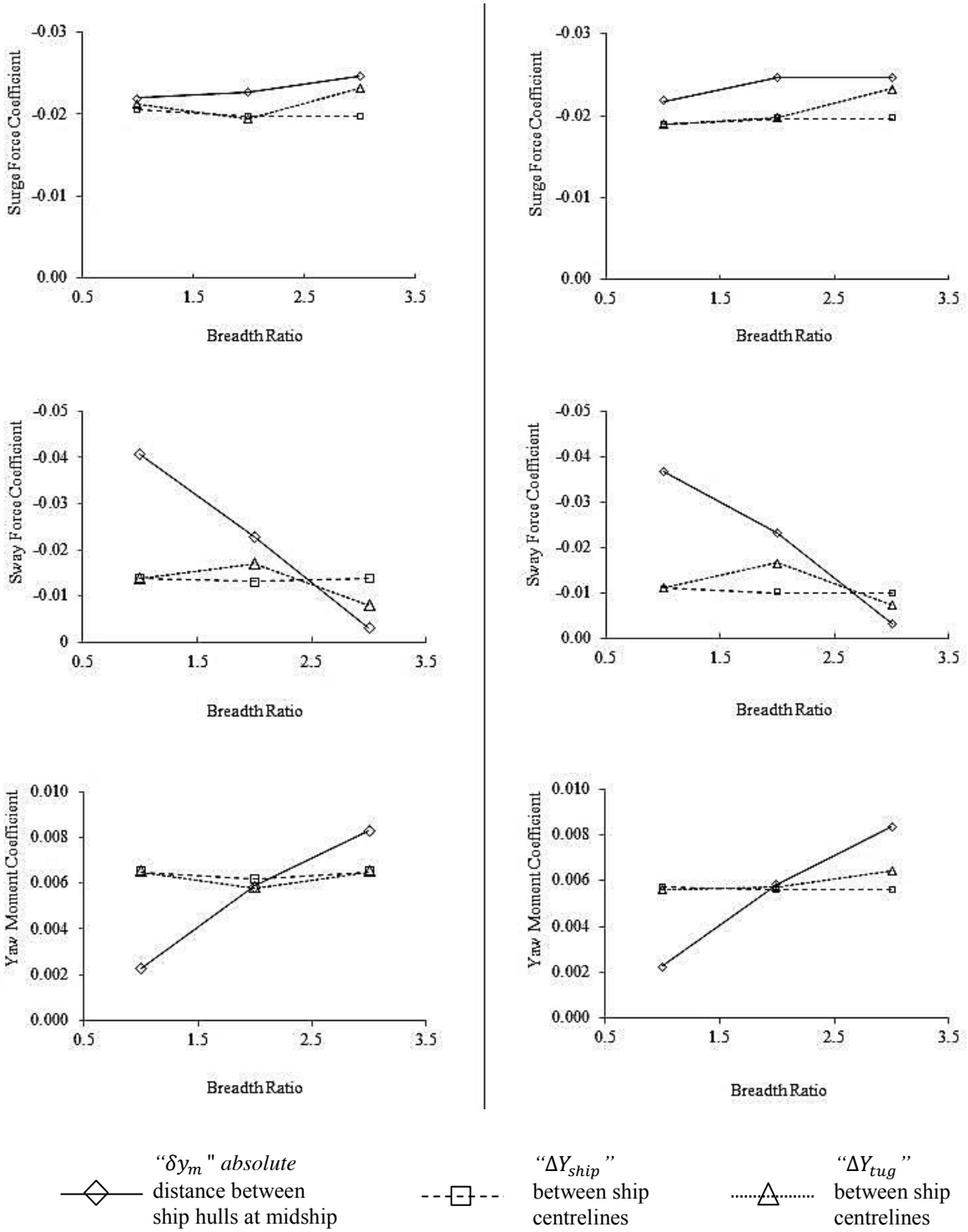

Figure 8: Surge force, sway force, and yaw moment coefficients of the tug determined for different δy_m, ΔY_{ship} and ΔY_{tug} for three full scale breadth ratios; *BR* = 1.14, 2.22, 3.17

As illustrated in Figure 8, the results determined using the ship's breadth to non-dimensionalise the lateral distance, i.e. ΔY_{ship}, showed good agreement in the interaction effects predicted for the three breadth ratios. The maximum discrepancies between the coefficients calculated were found to be 4%, 4%, and, 5% for surge force, sway force and yaw moment respectively for a ΔY_{ship_1} of 2.190 and up to 4%, 9% and 2% for a ΔY_{ship_2} of 2.276 respectively.

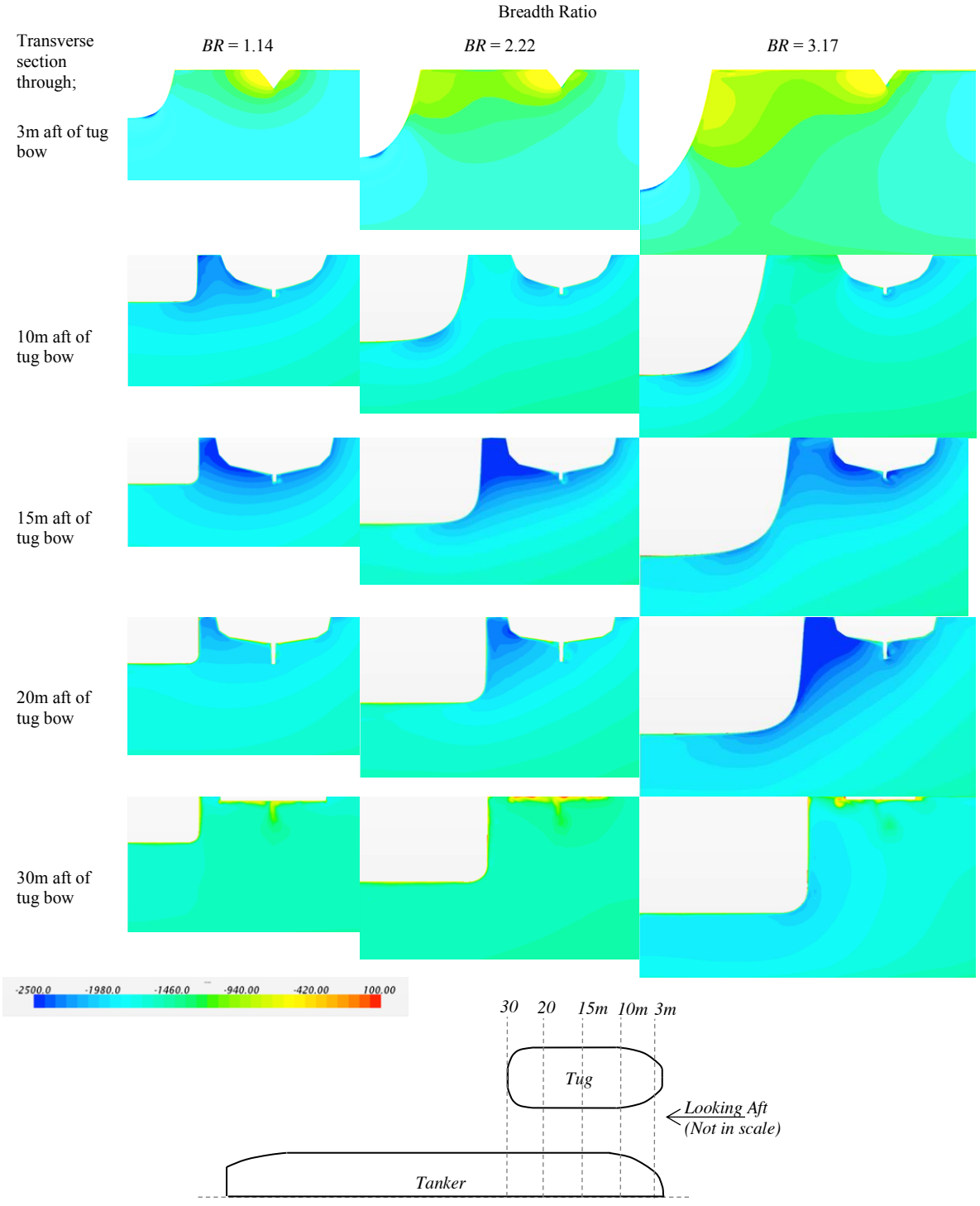

Figure 9: Pressure distribution plots on the transverse sections along the length of the tug at 3m, 10m, 15m, 20m, and 30m aft of the tug's bow for *BR* = 1.14, *BR* = 2.22, and *BR* = 3.17 when the lateral distance between vessel' hulls was maintained at δy_{m_1} = 0.913m.

These discrepancies were within the EFD and CFD uncertainties discussed in Section 5.2. In summary therefore, among the three lateral distance scaling methods investigated, the non-dimensioning method used with larger ship breadth, i.e. ΔY_{ship} was the most appropriate for interaction effect predictions. That is, it was the best for widely used ship-tug combinations that lie within and above the tested breadth ratio range. If it is required to use ΔY_{ship} for breadth ratios below this threshold where tugs are used to manoeuver with smaller ships, it is advisable to carry out further investigations to test its applicability.

6.2 PRESSURE PLOT VISUALISATION

CFD generated pressure plots are illustrated and discussed in the following two subsections. This is to highlight the significance of using non-dimensionalised values to predict the interaction effects of dissimilar sized vessels.

6.2 (a) Absolute lateral distance for scaling

Due to similar patterns in the results for the lateral distances (δy_m) of 0.913m and 0.975m (see Figure 8), only the results predicted for δy_m of 0.913m are discussed in this section. Figure 9 illustrates the full scale CFD pressure plots due to the interaction between the two hulls along transverse planes at tug lengths of 3m, 10m, 15m, 20m, and 30m aft of the tug's bow for *BR* of 1.14, 2.22, and, 3.17. As shown in Figure 9, near the tug bow (i.e. 3m aft of the bow), the pressure between the hulls increased significantly with the breadth ratio as a result of the increased tanker bow pressure region. For a *BR* of 3.17, the tanker bow pressure effect remains high up to the tug's midship (i.e. around 15m aft of the bow). This caused relatively high pressure between the hulls in comparison to the lesser breadth ratios.

Beyond midship however, pressure between the hulls reduced as the breadth ratio increased, as seen in Figure 9. At 20m aft of the tug's bow, a *BR* of 3.17 showed the least pressure between the hulls compared to the smaller breadth ratios due to the amplified venturi effect by the highly accelerated flow passing between the hulls. At the lower breadth ratio of 1.14, the low pressure region between the hulls was adversely affected due to a reduction in the accelerated flow between the hulls. This was influenced by the pressure around the tug's stern region as shown in the pressure plot at 20m aft of the tug's bow.

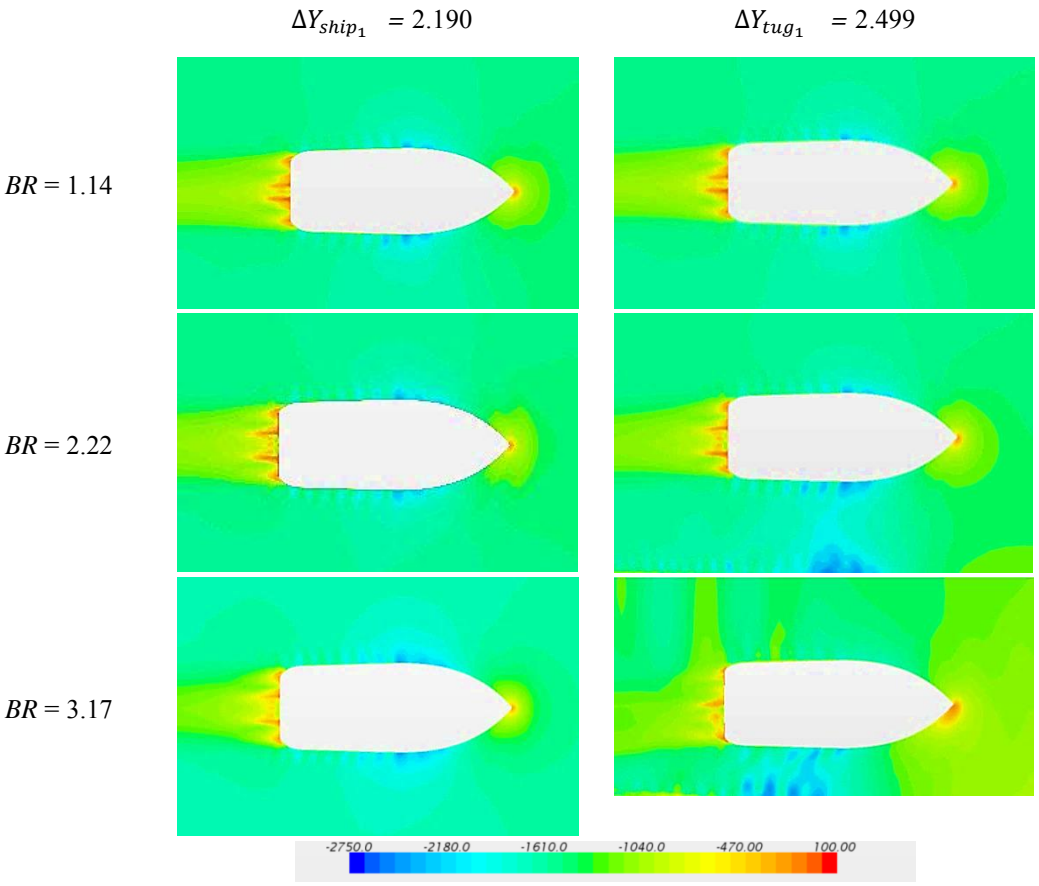

Figure 10: Pressure distribution plots on the tug for *BR* = 1.14, *BR* = 2.22, and *BR* = 3.17 for non-dimensionalised lateral distances of ΔY_{ship_1} = 2.190 and ΔY_{tug_1} = 2.499.

The results presented in Figure 9, at the aft-most point of the tug (i.e. 30m aft of the bow), show a decrease in pressure between the hulls with an increasing breadth ratio. It is therefore clear that the interaction effects predicted by using the absolute lateral distance for scaling were dominated by the larger ship size. This stresses the importance of having a suitable non-dimensioning method, as discussed in the previous section.

6.2 (b) Non-dimensionalised lateral distances for scaling

Figure 10 illustrates the pressure distribution around the tug when placed at different lateral distances to the tanker, as calculated by the two lateral distance non-dimensioning formula used in this study (eqns. 2 and 3). As seen in Figure 10, lateral distances calculated using the ΔY_{ship} formula (i.e. non-dimensionalised using the tanker breadth) showed similar pressure fields around the tug for all breadth ratios. This complimented the behaviour observed in the quantified interaction surge and sway forces and yawing moment coefficients presented in Figure 8, which displayed good agreement between different breadth ratios. For the ΔY_{tug} method, the pressure plots showed increasing pressure distribution differences as the breadth ratio increased. This supported the earlier quantitative findings in Figure 8, where larger discrepancies in the force coefficients between the different breadth ratios were observed.

These findings confirm that the non-dimensionalised lateral distance calculated using the breadth of the larger ship (i.e. ΔY_{ship}) was the most suitable method for comparing interaction effects acting on a tug during ship-assist manoeuvres. In other words it provided good scaling between different breadth ratios for the investigation of interaction effects between two dissimilar sized vessels.

7. CONCLUSION

Hydrodynamic interaction effects between two vessels operating in close proximity can affect the operational safety of those vessels. This is especially the case if the vessels are significantly different in size, for example when tugs assist large ships. The work presented here focused on the interaction effects on a tug operating around the forward shoulder of a tanker at different lateral distances during ship assist operations. It outlined an approach to non-dimensionalise lateral distances between vessels of dissimilar sizes. This is useful for predicting the interaction effects acting on the tug operating near ships of varying sizes and for correlating model scale and full scale interaction effects. This involved the verification of the approaches for non-dimensionalising lateral distances between the vessels for different full scale size vessels using validated CFD simulations.

The following are the key findings of this study:

- In order to compare the interaction effects between model scale and full scale data or to extrapolate model scale interaction effects to full scale, the lateral distance between the vessel centrelines should be non-dimensionalised using the large ship's breadth. The results obtained using this approach revealed a good agreement between the different breadth ratios investigated, i.e. 1.14 to 3.17, with the maximum differences for surge force, sway force, and yaw moment being 4%, 9%, and 5% respectively, which was within the calculated uncertainties. Thus, it is possible to use the interaction effects results from one ship-to-tug ratio to predict the safe operational distances for other ship-to-tug ratios when using the large ship breadth as the reference for the non-dimensioning method.
- Lateral distances calculated as a ratio of the tug's breadth did not provide satisfactory agreement between results for different breadth ratios. Rather, there was discrepancy of the forces as large as 41%. In the same way, using the absolute distance between the vessels was unsatisfactory as it doesn't account for vessel dimensions. This resulted in force and moment deviations of up to 268% across the breadth ratios considered in this study.
- When the tug was operating in close proximity to the forward quarter of the larger ship, interaction sway forces and yaw moments exhibited notable changes. As the breath ratio increased, the sway force declined, whereas the yaw moment rapidly increased. It is important that tug operators are aware of variations to the interaction effects when they operate in close proximity to ships of varying sizes, as it can lead to dangerous situations such as collisions or run-overs.

In future work, the location of a tug near a tanker will be extended to different lateral and longitudinal locations as well as different tug drift angles across a range of Froude numbers to develop comprehensive interaction effect plots for varying breadth ratios. These plots, together with the non-dimensioning method described here will enable tug operators to identify safe operational envelopes for a range of ship assist manoeuvers when they operate in close proximity to ships of varying sizes.

8. ACKNOWLEDGEMENTS

The authors would like to acknowledge the extensive support given by the AMC Model Test Basin staff during the experimental phase of this programme and DST Group for the use of the model carriage.

9. REFERENCES

1. ARTYSZUK, J. (2013). Types and Power of Harbour Tugs - The Latest Trends. Prace Naukowe Politechniki Warszawskiej - Transport, z.98. 1230-9265.

2. CD-ADAPCO (2015). User Manual of StarCCM+ Version 10.02.
3. CHEN, G. R. & FANG, M. C. (2001). Hydrodynamic Interactions Between Two Ships Advancing in Waves. Ocean Engineering, 28, 1053-1078. 0029-8018. http://dx.doi.org/10.1016/s0029-8018(00)00042-1
4. DAND, I. W. (1975). Some Aspects of Tug-Ship Interaction. The Fourth International Tug Convention, 1975 New Orleans, Louisiana, USA.
5. FALTER, J. (2010). Validation of a Potential Flow Code for Computation of Ship-Ship Interaction Forces with Captive Model Test Results. Ghent University, Belgium.
6. FONFACH, J. M. A. (2010). Numerical Study of the Hydrodynamic Interaction Between Ships in Viscous and Inviscid Flow. Instituto Superior Tecnico, Portugal.
7. FONFACH, J. M. A., SUTULO, S. & SOARES, C. G. (2011). Numerical Study of Ship to Ship Interaction Forces on the Basis of Various Flow Models. 2nd International Conference on Ship Manoeuvring in Shallow and Confined Water: Ship to Ship Interaction, 2011 Trondheim, Norway. RINA, 137-146
8. FORTSON, R. M. (1974). Interaction Force Between Ships. Massachusetts Institute of Technology, USA.
9. GEERTS, S., VANTORRE, M., ELOOT, K., HUIJSMANS, R. & FIERENS, N. (2011). Interaction Forces in Tug Operation. 2nd International Conference on Ship Manoeuvring in Shallow and Confined Water: Ship to Ship Interaction, 2011 Trondheim, Norway.
10. HENSEN, H. (2003). Tug Use in Port: A Practical Guide, Nautical Institute. 9781870077392.
11. HENSEN, H. (2012). Safe Tug Operation: Who Takes the Lead? International Tug & OSV, 2012, 70-76.
12. ITTC (2002). Testing and Extrapolation Methods - Resistance Uncertainty Analysis. International Towing Tank Conference.
13. JAYARATHNE, B. N., RANMUTHUGALA, D., CHAI, S. & FEI, G. (2014). Accuracy of Potential Flow Methods to Solve Real-time Ship-Tug Interaction Effects within Ship Handling Simulators. International Journal on Marine Navigation and Safety of Sea Transportation, 8, 497-504. 2083-6473. http://dx.doi.org/10.12716/1001.08.04.03
14. JAYARATHNE, B. N., RANMUTHUGALA, D., LEONG, Z. Q., CHAI, S. & FEI, G. (2017). Numerical and Experimental Prediction of Hydrodynamic Interaction Effects Acting on Tugs during Ship Manoeuvres. Journal of Marine Science and Technology (Accepted for publication). 1023-2796.
15. LATAIRE, E., VANTORRE, M., DELEFORTRIE, G. & CANDRIES, M. (2012). Mathematical Modelling of Forces Acting on Ships During Lightering Operations. Ocean Engineering, 55, 101-115. 0029-8018. https://doi.org/10.1016/j.oceaneng.2012.07.029
16. LEONG, Z. Q., RANMUTHUGALA, D., PENESIS, I. & NGUYEN, H. (2014). RANS-Based CFD Prediction of the Hydrodynamic Coefficients of DARPA SUBOFF Geometry in Straight-Line and Rotating Arm Manoeuvres. Transactions RINA: Part A1- International Journal Maritime Engineering. 1479-8751.
17. LU, H., YANG, C. & LOHNER, R. (2009). Numerical Studies of Ship-Ship Interactions in Extreme Waves. Grand Challenges in Modeling & Simulation 2009 USA. 43-55
18. NEWTON, R. N. (1960). Some Notes on Interaction Effects Between Ships Close Aboard in Deep Water. First Symposium on Ship Maneuverability, 1960 Washington D. C.: U.S. Government Printing Office,
19. PINKSTER, J. A. & BHAWSINKA, K. (2013). A Real-time Simulation Technique for Ship-Ship and Ship-Port Interactions. 28th International Workshop on Water Waves and Floating Bodies (IWWWFB 2013), 2013 L'Isle sur la Sorgue, France.
20. SIMONSEN, C. D., NIELSEN, C. K., OTZEN, J. F. & AGDRUP, K. (2011). CFD Based Prediction of Ship-Ship Interaction Forces on a Tug Beside a Tanker. 2nd International Conference on Ship Manoeuvring in Shallow and Confined Water: Ship to Ship Interaction, 2011 Trondheim, Norway.
21. STERN, F., WILSON, R. V., COLEMAN, H. W. & PETERSON, E. G. (2001). Comprehensive Approach to Verification and Validation of CFD Simulations - Part 1: Methodology and Procedures. Journal of Fluids Engineering, 123, 793-802. 0098-2202. https://doi.org/10.1115/1.1412235
22. TUCK, E. O. & NEWMAN, J. N. (1974). Hydrodynamic Interactions Between Ships. 10th Symposium on Naval Hydrodynamics, 1974 USA. 35-69
23. VANTORRE, M., VERZHBITSKAYA, E. & LAFORCE, E. (2002). Model Test Based Formulations of Ship-Ship Interaction Forces. Ship Technology Research, 49, 124-141. 0937-7255.
24. ZOU, L. & LARSSON, L. (2013). Numerical Predictions of Ship-to-Ship Interaction in Shallow Water. Ocean Engineering, 72, 386–402. 0029-8018.